

# Hard X-ray emission and $^{44}\text{Ti}$ line features of Tycho Supernova Remnant

Wei Wang<sup>1</sup> and Zhuo Li<sup>2,3</sup>

<sup>1</sup> *National Astronomical Observatories, Chinese Academy of Sciences, 20A Datun Road, Chaoyang District, Beijing 100012, China; wangwei@bao.ac.cn*

<sup>2</sup> *Department of Astronomy and Kavli Institute for Astronomy and Astrophysics, Peking University, Beijing 100871, China; zhuo.li@pku.edu.cn*

<sup>3</sup> *Key Laboratory for the Structure and Evolution of Celestial Objects, Chinese Academy of Sciences, Kunming 650011, China*

## ABSTRACT

A deep hard X-ray survey of the INTEGRAL satellite first detected the non-thermal emission up to 90 keV in the Tycho supernova (SN) remnant. Its 3 – 100 keV spectrum is fitted with a thermal bremsstrahlung of  $kT \sim 0.81 \pm 0.45$  keV plus a power-law model of  $\Gamma \sim 3.01 \pm 0.16$ . Based on the diffusive shock acceleration theory, this non-thermal emission, together with radio measurements, implies that Tycho remnant may not accelerate protons up to  $>\text{PeV}$  but hundreds TeV. Only heavier nuclei may be accelerated to the cosmic ray spectral “knee”. In addition, we search for soft gamma-ray lines at 67.9 and 78.4 keV coming from the decay of radioactive  $^{44}\text{Ti}$  in Tycho remnant by INTEGRAL. A bump feature in the 60-90 keV energy band, potentially associated with the  $^{44}\text{Ti}$  line emission, is found with a marginal significance level of  $\sim 2.6 \sigma$ . The corresponding  $3 \sigma$  upper limit on the  $^{44}\text{Ti}$  line flux amounts to  $1.5 \times 10^{-5}$  ph cm<sup>-2</sup> s<sup>-1</sup>. Implications on the progenitor of Tycho SN, considered to be the prototype of type Ia SN, are discussed.

*Subject headings:* supernovae: individual (Tycho) - ISM: supernova remnants - Gamma Rays: Observations - cosmic rays

## 1. Introduction

Tycho supernova (SN 1572) is a historical supernova occurring in early November of 1572 in the constellation Cassiopeia region. This supernova explosion event was suggested to be the Type Ia supernova, but no convinced evidence was found (e.g., Ruiz-Lapuente

2004). Recent spectral analysis of the light echo from the explosion (Krause et al. 2008) has confirmed that the event was a Type Ia supernova. Measurements of the distance of the Tycho remnant still have large uncertainties. The kinematic distance obtained by observing HI absorption toward the Tycho remnant gives a large distance range of 1.7 – 5.0 kpc (Albinson et al. 1986; Schwarz et al. 1995; Tian & Leahy 2011). Modeling of the observed  $\gamma$ -ray emission from Tycho suggests a distance greater than 3.3 kpc (Völk et al. 2008). A direct distance estimate is also given by X-ray ejecta proper-motion observations by Chandra and Suzaku which give a distance of  $4 \pm 1$  kpc (Hayato et al. 2010).

Supernova remnants (SNRs) are generally thought to be the promising sites of producing high energy cosmic rays (CRs) up to the energies of  $> 10^{15}$  eV. The accelerated electrons and protons can produce non-thermal emissions observed from radio to gamma-ray bands. Non-thermal emission from the Tycho SNR has been detected in radio, X-rays and gamma-rays. Radio images also show a shell-like morphology with enhanced emission along the northeastern edge of the remnant (Dickel et al. 1991; Stroman & Pohl 2009). Soft X-ray images by Chandra reveal the non-thermal X-ray emission concentrated on the SNR rim (Hwang et al. 2002; Bamba et al. 2005; Warren et al. 2005), which has been interpreted as the evidence of electron acceleration. The first evidence for hard X-ray emission from the Tycho SNR was reported by HEAO 1 (Pravdo et al. 1979) which suggested a photon index of  $\sim 2.72$  from 5 – 25 keV. RXTE also reported a hard X-ray continuum up to 20 keV with a photon index of  $\sim 3$  (Petre et al. 1999). Recent detection by Suzaku HXD-PIN detector up to 28 keV implies the possible presence of accelerated electron up to the energy at least  $\sim 10$  TeV (Tamagawa et al. 2009). The Suzaku spectrum of the Tycho SNR from 13 – 28 keV was described by a power-law model of photon index  $\Gamma \sim 2.8 \pm 0.5$ . In gamma-ray bands, Fermi/LAT detected the GeV emission from the Tycho SNR with a photon index of  $\Gamma \sim 2.3 \pm 0.3$  (Giordano et al. 2012). And the VERITAS Cherenkov telescope succeeded in measuring its TeV emission up to 10 TeV (Acciari et al. 2011), with a photon index of  $\Gamma \sim 1.95 \pm 0.81$ .

The accelerated electrons emit synchrotron radiation observed from radio to X-ray bands. But the non-thermal emissions in soft X-ray bands generally are difficult to be discriminated from thermal components in SNRs. In hard X-ray bands ( $> 10$  keV), the observations are a direct way to probe the non-thermal emission properties, constraining the accelerating ability of SNRs. The hard X-ray properties of the Tycho SNR have never been studied in detail due to the poor sensitivity above 20 keV of past missions. Suzaku made a detection of the hard X-ray emission up to 28 keV (Tamagawa et al. 2008), but we do not know its spectral characteristics at higher energies. The instruments onboard INTEGRAL have a better sensitivity above 20 keV up to several hundred keV and would provide new information on the non-thermal emission properties of the supernova remnant.

In addition, hard X-ray studies on SNRs could search for the hard X-ray lines from radioactive  $^{44}\text{Ti}$  at  $\sim 68$  and  $78$  keV.  $^{44}\text{Ti}$  is a short-lived radioactive isotope with a mean life of 85 years (Admad et al. 2006). In theories, the most plausible cosmic environment for production of  $^{44}\text{Ti}$  is the  $\alpha$ -rich freeze-out from high-temperature burning near the nuclear statistical equilibrium (Woosley et al. 1973; Timmes et al. 1996). This required high values for the entropy can be found in supernovae. It is generally believed that core-collapse supernovae dominate the production of radioactive  $^{44}\text{Ti}$  (Timmes et al. 1996). The decays of  $^{44}\text{Ti}$  can emit four lines at energies of 4.1, 67.9, 78.4 and 1157 keV, where the line flux at 4.1 keV is about 20% of the other lines, and the flux of 67.9 keV is about 93% the flux at 78.4 keV. Previously, the 67.9, 78.4 and 1157 keV lines from Cas A were reported (Iyudin et al. 1994, 1999; Vink et al. 2001; Renaud et al. 2006a, 2006b). Two hard X-ray lines at 67.9, 78.4 keV from SN 1987A were recently discovered (Grebenev et al. 2012). These two supernovae are known to be of core-collapse origin. Tentative detections of the 1157 keV line from the Vela Junior (Iyudin et al. 1998) and the 4.1 keV line from the G1.9+0.3 (Borkowski et al. 2010) were also reported.

Generally a Type Ia supernova like Tycho is not thought to produce a large amount of  $^{44}\text{Ti}$ . However, great uncertainty still surrounds the central driver of these Type Ia explosions, just what kind of star explodes. Is the white dwarf that blows up near the upper limit allowed by nature (the "Chandrasekhar mass"), or lighter, and does the explosion result from the slow accretion of matter from a companion star or the dynamic merger of two white dwarfs? An important diagnostic of the models is the nucleosynthesis that they produce. In the Chandrasekhar mass explosions, the fuel is a mixture of carbon and oxygen and the burning produces a distinctive set of iron-group and intermediate-mass elements. Sub-Chandrasekhar mass models, on the other hand, have a component of explosive helium burning which produces different set, rich in the isotopes of calcium, titanium. Depending upon the kind of dwarfs that come together, merging white dwarfs can give both. Therefore, searching for the  $^{44}\text{Ti}$  lines in the Tycho remnant is an important tool to probe the nature of the progenitor in this Type Ia supernova. COMPTEL three-year search for the  $^{44}\text{Ti}$  signals of galactic sources gave an upper limit ( $2\sigma$ ) of  $2 \times 10^{-5}$  ph cm $^{-2}$  s $^{-1}$  (Dupraz et al. 1997; Iyudin et al. 1999). Early INTEGRAL/IBIS observations of the  $^{44}\text{Ti}$  hard X-ray lines also implies an upper limit ( $3\sigma$ ) of  $1.5 \times 10^{-5}$  ph cm $^{-2}$  s $^{-1}$  (Renaud et al. 2006b). In this work we will report our detections of the hard X-ray emission up to 100 keV and searching for  $^{44}\text{Ti}$  emission lines in Tycho remnant with INTEGRAL observations.

## 2. INTEGRAL Observations and data analysis

INTEGRAL is an ESA’s currently operational space-based hard X-ray/soft gamma-ray telescope covering a wide energy range of 3 keV – 8 MeV (Winkler et al. 2003). In this work, we have used two main instruments aboard INTEGRAL, the imager IBIS (Ubertini et al. 2003) and X-ray monitors JEM-X (Lund et al. 2003). The hard X-ray data are mainly collected with the low-energy array called IBIS-ISGRI (INTEGRAL Soft Gamma-Ray Imager) which consists of a pixellated  $128 \times 128$  CdTe solid-state detector that views the sky through a coded aperture mask (Lebrun et al. 2003). IBIS-ISGRI has a  $12'$  (FWHM) angular resolution and arcmin source location accuracy in the energy band of 15 – 200 keV. JEM-X as the small X-ray detector collects the lower energy photons from 3 – 35 keV which is used to constrain the lower hard X-ray band spectral properties of Tycho SNR.

The Tycho SNR is frequently observed during the INTEGRAL surveys on the Cassiopeia region. We use the available archival data from the INTEGRAL Science Data Center (ISDC) where the Tycho SNR was within  $\sim 12$  degrees of the pointing direction of INTEGRAL/IBIS observations. The total on-source time obtained in our analysis is about 4.9 Ms after excluding the bad data due to solar flares and the INTEGRAL orbital phase near the radiation belt of the Earth. The analysis was done with the standard INTEGRAL off-line scientific analysis (OSA, Goldwurm et al. 2003) software, ver. 10. Individual pointings in all collected IBIS data processed with OSA 10 were mosaicked to create the sky images for the source detection in the energy ranges of 20 – 60 keV and 60 – 90 keV. The Tycho SNR was detected by IBIS with significance levels of  $11.6\sigma$  and  $\sim 5.0\sigma$  in two energy ranges respectively (see middle and right panels in Fig. 1). JEM-X imagers have a much smaller field of view (requiring observing off-axis angle  $< 5^\circ$ ) and a relatively low sensitivity because of small detector area, the total on-source time for the Tycho SNR is about 460 ks. The mosaic map around Tycho detected JEM-X is also shown in Fig. 1 (left panel). The detection significance level is about  $9.8\sigma$  in the range of 3 – 10 keV.

The spectral extraction processes for IBIS and JEM-X are carried out individually. Tycho remnant is about  $8'$  in diameter in the sky. This size is smaller than the angular resolution of IBIS-ISGRI ( $12'$ ), but larger than the angular resolution of JEM-X ( $3'$ ). For IBIS, the spectral extraction was done using the software script *ibis\_science\_analysis* up to the *SPE* level with the input source catalog. Above  $\sim 90$  keV, only upper limits can be given by the ISGRI detector. For the spectral analysis on Tycho SNR using JEM-X, we have made use of the *mosaic\_spec* script to extract the spectrum from 3 – 35 keV by assuming a source size of  $\sim 8'$ . The spectral data points are directly derived from the mosaic images of JEM-X in four energy bands: 3 – 6 keV, 6 – 10 keV, 10 – 16 keV, and 16 – 35 keV.

### 3. Hard X-ray spectral characteristics of Tycho SNR

We first derived the hard X-ray spectrum of the Tycho remnant obtained by IBIS which has a very long exposure on the source. In Fig. 2, we present the spectra of Tycho from 18 – 150 keV in two time intervals when IBIS carried out deep observations on the source, one in 2005 and the other from 2010 – 2011. Both two spectra are fitted with a simple power-law model. There exists a feature around 60 – 90 keV in both spectra. These features may be attributed to the  $^{44}\text{Ti}$  line signal. To probe the bump feature near 60 – 90 keV in details, we re-extracted the IBIS hard X-ray spectra from 18 – 200 keV using all the available data with smaller energy bins from 30 – 90 keV. The lower energy band data points can be used to constrain the continuum better, so that the JEM-X spectrum of Tycho is extracted for the analysis together in the followings.

The extracted hard X-ray spectra from 3 – 35 keV from JEM-X and 18 – 200 keV from IBIS for the Tycho SNR are displayed together in Fig. 3. The spectrum from 3 – 200 keV is initially fitted with a thermal bremsstrahlung of  $kT \sim 0.92 \pm 0.48$  keV plus a power-law model of  $\Gamma \sim 3.02 \pm 0.14$ , reduced  $\chi^2 = 1.251$  (22 *d.o.f.*). The derived hard X-ray non-thermal emission spectral property is still consistent with the result by the Suzaku observations from 13 – 28 keV (Tamagawa et al. 2009). The derived continuum flux from 3 – 100 keV is about  $8.5 \times 10^{-11}$  erg cm $^{-2}$  s $^{-1}$ , corresponding to a hard X-ray luminosity of  $\sim 2 \times 10^{35} d_4^2$  erg s $^{-1}$ .

However, there is still some excess around 60-90 keV in the residuals from this continuum best-fit model, which might be attributed to the  $^{44}\text{Ti}$  line emission. Thus we re-fit the spectra from 3 – 200 keV with a continuum model (a thermal bremsstrahlung and a power law) plus two gaussian lines. The line positions in the fitting is fixed to be at 67.9 and 78.4 keV, and the line width is set to be zero due to the low spectral resolution of IBIS/ISGRI around 70 keV ( $\sim 8\%$ ). In addition, to improve the statistical significance of hard X-ray line detection, we also fix the line flux ratio during the fitting:  $F_{68} = 0.93F_{78}$ . Then we derive  $kT \sim 0.81 \pm 0.45$  keV, and the photon index of  $\Gamma \sim 3.01 \pm 0.16$  with the mean line flux of  $F_{78} \sim (1.3 \pm 0.5) \times 10^{-5}$  ph cm $^{-2}$  s $^{-1}$  (reduced  $\chi^2 = 0.422$  /21 *d.o.f.*). The significance of the detection is still low ( $\sim 2.6\sigma$ ) with the present measurements, so that we also give a  $3\sigma$  upper limit of  $1.5 \times 10^{-5}$  ph cm $^{-2}$  s $^{-1}$  on the  $^{44}\text{Ti}$  line emission in Tycho. Anyway, this marginal detection of the  $^{44}\text{Ti}$  signal in this Type Ia supernova remnant will be interesting and help us to probe the progenitor of this remnant.

## 4. Discussion

### 4.1. $^{44}\text{Ti}$ amount in Tycho remnant

The creation of  $^{44}\text{Ti}$  in a supernova requires the presence of a large mass fraction of helium heated briefly to temperatures in excess of about 2 billion K. These conditions exist either when material in nuclear statistical equilibrium is rapidly quenched at such a low density that the helium fails to fully reassemble into iron-group elements, the so called “alpha-rich freeze out” (Woosley et al. 1973), or when a detonation wave passes through a helium-rich composition at typical white dwarf densities. The alpha-rich freeze out can happen either in a massive star, where it occurs in the deepest layers to be ejected (Timmes et al. 1996), or in the carbon-rich layers of a Type Ia supernova (Iwamoto et al. 1999; Maeda et al. 2010; Seitenzahl et al. 2013). In the latter case, the synthesis of  $^{44}\text{Ti}$  is relatively small due to the high density during the freeze-out. Helium detonation occurs only in Type Ia supernovae and there the production of  $^{44}\text{Ti}$  can sometimes be very substantial (Woosley & Weaver 1994; Timmes et al. 1996).

These general considerations translate into typical  $^{44}\text{Ti}$  yields for current models for Type Ia supernovae. For Type Ia supernovae resulting from carbon deflagration and detonation in white dwarfs near the Chandrasekhar mass, the yield is quite low, typically  $(0.2 - 1.6) \times 10^{-5} M_{\odot}$  based on the multi-dimensional simulations (Maeda et al. 2010; Seitenzahl et al. 2013) with the lower values more typical of the most recent three-dimensional (3D) models. Sub-Chandrasekhar mass models for Type Ia supernovae, on the other hand, are prolific sources of  $^{44}\text{Ti}$  and it has long been thought that the production of the nucleus  $^{44}\text{Ca}$  in nature occurs chiefly in this kind of explosion (Timmes et al. 1996). These models are characterized by a shell of helium of about  $0.05 - 0.2 M_{\odot}$  atop a carbon-oxygen dwarf of  $0.7$  to  $1.0 M_{\odot}$ . The detonation of the helium induces a secondary detonation of the carbon and the entire white dwarf explodes leaving no remnant. Recent calculations (Woosley & Kasen 2011) of this sort of model give  $^{44}\text{Ti}$  yields in the range  $(5 - 500) \times 10^{-5} M_{\odot}$ . While we can find no published nucleosynthesis studies, we also expect that merging white dwarfs in which one of the components is a helium white dwarf would give similarly high yields provided that some portion of the helium detonates (Dan et al. 2012).

Using the observed line flux, the  $^{44}\text{Ti}$  yield synthesized in the supernova can be estimated:

$$M_{44Ti} \approx 4\pi d^2 44m_p \tau \exp(t/\tau) F_{44Ti}, \quad (1)$$

where  $d$  is the distance of the Tycho remnant,  $m_p$ , the proton mass,  $\tau$ , the characteristic time of the  $^{44}\text{Ti}$  decay chain,  $t$ , the time since the explosion, and  $F_{44Ti}$ , the flux of the  $^{44}\text{Ti}$  emission line. As discussed in the introduction, we take the most likely distance distribution

of the Tycho supernova remnant to be 1.7 – 5.0 kpc in this work.

An upper limit of the  $^{44}\text{Ti}$  line flux in Tycho is derived to be  $1.5 \times 10^{-5}$  ph cm $^{-2}$  s $^{-1}$  ( $3\sigma$ ). Fig. 4 shows the  $^{44}\text{Ti}$  yield upper limit (the solid line) we have observed in Tycho remnant plotted against the uncertain distance to the remnant according to Eq. (1). The region between two red arrows is the estimated  $^{44}\text{Ti}$  yield limit for distances in the most probable range, 1.7 – 5.0 kpc, based on the measured  $^{44}\text{Ti}$  line flux upper limit at 68 and 78 keV in Tycho. The estimated  $^{44}\text{Ti}$  yield ranges according to the simulation results of both the standard Chandrasekhar mass models and sub-Chandrasekhar mass models are also plotted. The present observed upper limit of the  $^{44}\text{Ti}$  yield in Tycho is still consistent with both two explosion models for the Type Ia supernovae.

#### 4.2. Non-thermal hard X-ray emission up to 100 keV

Based on the diffusive shock acceleration (DSA) theory we discuss the acceleration ability of Tycho SNR shock, using the hard X-ray observation up to 100 keV, that probing the cutoff of the electron spectrum.

The acceleration of electrons suffers from radiative energy loss. The maximum synchrotron photon energy where the electron acceleration and synchrotron cooling times are equal is  $h\nu_{\text{cutoff}} \sim 0.15\xi(E_{e,\text{max}})^{-1}v_8^2\text{keV}$  (e.g., Katz & Waxman 2008), where  $\xi(E) \geq 1$  is the ratio of the diffusion coefficient to the Bohm diffusion one and could be energy dependent, and  $v_8$  is the SNR shock velocity in units of  $10^8$  cm s $^{-1}$ . The measurements of proper motion of ejecta in Tycho SNR usually give an expansion velocity of  $v \sim 5000$  km/s (Hayato et al. 2008; Katsuda et al. 2010), so the synchrotron cutoff is  $\sim 4\xi^{-1}\text{keV}$ , while the detected 100 keV emission in Tycho is well above. Recently Zirakashvili & Aharonian (2007; 2010) investigated the spectral shape of the shock-accelerated electrons subject to synchrotron cooling in the context of DSA theory. They provided useful approximations for the subsequent synchrotron spectral shape, which is a slow function other than sharp cutoff. Using their approximation (eq. 37 in Zirakashvili & Aharonian 2007), in order for the 3–100 keV emission to be statistically compatible to a power law with photon index of  $\sim 3$ , the cutoff should be  $\sim 3$  keV $^1$ . Therefore the highest energy electrons are accelerated close to the Bohm limit,  $\xi(E_{e,\text{max}}) \sim 1.3(v/5000\text{km s}^{-1})^2(h\nu_{\text{cutoff}}/3\text{keV})^{-1}$ , consistent with the fact that the approximation used is derived for the Bohm diffusion regime.

---

<sup>1</sup>The cutoff energy in eq. (37) of Zirakashvili & Aharonian (2007) is not exactly the same as  $h\nu_{\text{cutoff}}$  here but different by about 20%. However given the uncertainty in the DSA theory and for purpose of order of magnitude estimate we neglect the difference.

The postshock magnetic field can be constrained with the multi-band synchrotron spectrum. If the accelerated electron distribution follows a single power law, the downstream electron distribution is a broken power law, with a cooling break in the synchrotron spectrum corresponding to where the synchrotron cooling time is equal to the SNR age,  $h\nu_{\text{cool}} \approx 3B_{-4}^{-3}t_{\text{kyr}}^{-2}$  eV (e.g., Katz & Waxman 2008). At this break the synchrotron spectral index steepens by a half. Given the normalization and spectral index of radio emission from Tycho (Kothes et al. 2006), the cooling break occurs around  $\sim 10$  eV in order for the extrapolated flux to match the observed X-ray flux of Suzaku and INTEGRAL (see also Fig. 10 in Morlino & Caprioli 2012). Given  $h\nu_{\text{cool}} \sim 10$  eV and  $t \approx 440$  yr, the postshock magnetic field is then derived to be  $B \sim 120(h\nu_{\text{cool}}/10\text{eV})^{-1/3}\mu\text{G}$ , insensitive to  $\nu_{\text{cool}}$  and comparable to that derived from the observation of the X-ray rim (e.g., Warren et al. 2005)<sup>2</sup>.

The acceleration of nuclei suffers mainly from the limited SNR age, thus the maximum nuclei energy is  $E_{\text{max}} \approx 60Z\xi(E_{\text{max}})^{-1}B_{-4}v_8^2t_{\text{kyr}}$  TeV (e.g., Katz & Waxman 2008), where  $Z$  is the nuclear charge number. Using the above constraints of  $B$  and  $\xi(E_{e,\text{max}})$  by observations, the maximum cosmic ray energy can be expressed as

$$E_{\text{max}} \approx 640Z \frac{\xi(E_{e,\text{max}})}{\xi(E_{\text{max}})} \left( \frac{h\nu_{\text{cutoff}}}{3\text{keV}} \right) \left( \frac{h\nu_{\text{cool}}}{10\text{eV}} \right)^{-1/3} \text{TeV}, \quad (2)$$

only with the unknown parameter of  $\xi(E_{e,\text{max}})/\xi(E_{\text{max}})$ . With the constraint of  $B$  the 100 keV emitting electrons have high energy of  $E > 200$  TeV, not far from the above value. The fact that the 3–100 keV spectrum is compatible to the case of Bohm diffusion regime suggests  $\xi(200\text{TeV}) \sim 1$ . Since  $\xi$  may not vary sensitively with particle energy, we have  $\xi(E_{\text{max}}) \sim 1$  and  $\xi(E_{e,\text{max}})/\xi(E_{\text{max}}) \sim 1$ , although  $\xi(E_{e,\text{max}})/\xi(E_{\text{max}}) \ll 1$  could not be ruled out. There are hints from measurements of the expansion rate that Tycho is currently transiting into the Sedov-Taylor phase (e.g., Katsuda et al. 2010). During the transition SNRs are expected to produce the highest energy cosmic rays in their whole lives. In summary, Tycho may not accelerate protons up to the PeV scale; however, it is possible that light nuclei with  $Z \gtrsim$  a few may be accelerated to the PeV scale, but impossible to be far above PeV. Similar conclusion has been reached by e.g., Bell (2013) in a specific model.

## 5. Conclusion

This work studied the hard X-ray properties of the Tycho SNR using INTEGRAL deep observations from 2003 – 2011. We detected Tycho firstly up to 90 keV. The X-ray spectrum

---

<sup>2</sup>Note that by the similar argument Morlino & Caprioli (2012) derived an even somewhat higher magnetic field of  $200\mu\text{G}$ , leading to higher cosmic ray energy  $E_{\text{max}}$ .



from 3 – 100 keV can be described by a thermal bremsstrahlung of  $kT \sim 0.8$  keV and a power-law model of  $\Gamma \sim 3$ . A bump feature around 60 – 90 keV is found in the spectrum which is possibly the signal of  $^{44}\text{Ti}$  emission lines at 68 and 78 keV. The gaussian line profile is used to fit the two lines, and we find the marginal detection of the  $^{44}\text{Ti}$  lines at a significance level of  $\sim 2.6\sigma$ . Thus we find a  $3\sigma$  upper limit of  $1.5 \times 10^{-5}$  ph cm $^{-2}$  s $^{-1}$  for the  $^{44}\text{Ti}$  lines.

The detected non-thermal emission up to  $\sim 90$  keV in the Tycho SNR also suggests that the remnant could accelerate protons to at least  $\sim 200$  TeV, but not up to the PeV scale. The light nuclei with  $Z \gtrsim$  a few may be accelerated to the PeV scale, around the cosmic ray spectral “knee” region. This implies that the composition of cosmic rays at the “knee” is not dominated by protons but by light nuclei, if normal SNRs are the origins of cosmic rays at the “knee”.

We are grateful to the referee for the critical and fruitful comments and Stan Woosley for discussions on nucleosynthesis in supernovae. This work is supported by the NSFC (No. 11073030, 11273005), the SRFDP (20120001110064), the CAS Open Research Program of Key Laboratory for the Structure and Evolution of Celestial Objects, and the National Basic Research Program (973 Program) of China (2014CB845800).

## REFERENCES

- Acciari, V. A. et al. 2011, ApJL, 730, L20
- Admad, I. et al., 2006, Phys. Rev. C. 74, 065803
- Albinson, J. S. et al., 1986, MNRAS, 219, 427
- Bamba, A. et al., 2005, ApJ, 621, 793
- Bell, A. 2013, arXiv:1311.5779
- Borkowski, K.J. et al. 2010, ApJL, 724, L161
- Dan, M.; Rosswog, S.; Guillochon, J.; Ramirez-Ruiz, E., 2012, MNRAS, 422, 2417
- Dickel, J. R., van Breugel, W. J. M., & Strom, R. G. 1991, AJ, 101, 2151
- Dupraz, C. et al. 1997, A&A, 324, 683
- Giordano, F. et al., 2012, ApJL, 744, L2

- Goldwurm, A. et al., 2003, *A&A*, 411, L223
- Hayato, A. et al., 2010, *ApJ*, 725, 894
- Hwang, U., Decourchelle, A., Holt, S. S., Petre, R. 2002, *ApJ*, 581, 1101
- Iwamoto, K. et al., 1999, *ApJS*, 125, 439
- Iyudin, A.F. et al., 1994, *A&A*, 368, L1
- Iyudin, A.F. et al., 1998, *Nature*, 396, 142
- Iyudin, A.F. et al., 1999, *Astrophys. Lett. & Comm.*, 38, 383
- Katz, B., & Waxman, E. 2008, *J. Cosmology Astropart. Phys.*, 1, 18
- Katzuda, S. et al., 2010, *ApJ*, 709, 1387
- Kothes, R. et al. 2006, *A&A*, 457, 1081
- Lund, N. et al., 2003, *A&A*, 411, L231
- Maeda, K. et al., 2010, *ApJ*, 712, 624
- Morlino, G., & Caprioli, D. 2012, *A&A*, 538, A81
- Petre, R., Allen, G. E., Hwang, U. 1999, *Astron. Nachr.*, 320, 199
- Pravdo, S. H., Smith, B. W. 1979, *ApJ*, 234, L195
- Renaud, M. et al., 2006a, *ApJL*, 647, L41
- Renaud, M. et al., 2006b, *New Astronomy Reviews*, 50, 540
- Ruiz-Lapuente, P., 2004, *ApJ*, 612, 357
- Ruiz-Lapuente, P.; Comeron, F.; M'endez, J.; et al., 2004, *Nature*, 431, 1069
- Schwarz, U. J. et al., 1995, *A&A*, 299, 193
- Seitenzahl, Ivo R. et al., 2012, *MNRAS*, 429, 1156
- Stroman, W., & Pohl, M. 2009, *ApJ*, 696, 1864
- Tamagawa, T. et al., 2009, *PASJ*, 61, S167
- Tian, W. W.; Leahy, D. A., 2011, *ApJL*, 729, L15

- Timmes, F.X.; Woosley, S.E.; Hartmann, D.H.; Hoffman, R.D., 1996, *ApJ*, 464, 332
- Ubertini, P. et al., 2003, *A&A*, 411, L131
- Vink, J. et al. 2001, *ApJL*, 560, L79
- Völk, H. J.; Berezhko, E. G.; Ksenofontov, L. T., 2008, *A&A*, 483, 529
- Warren, J. S., et al. 2005, *ApJ*, 634, 376
- Winkler, C. et al., 2003, *A&A*, 411, L1
- Woosley, S. E.; Arnett, W. D.; Clayton, D.D., 1973, *ApJS*, 26, 231
- Woosley, S. E.; Weaver, T. A., 1994, *ApJ*, 423, 371
- Woosley, S. E.; Kasen, D., 2011, *ApJ*, 734, 38
- Zirakashvili, V. N., & Aharonian, F. 2007, *A&A*, 465, 695
- Zirakashvili, V. N., & Aharonian, F. A. 2010, *ApJ*, 708, 965

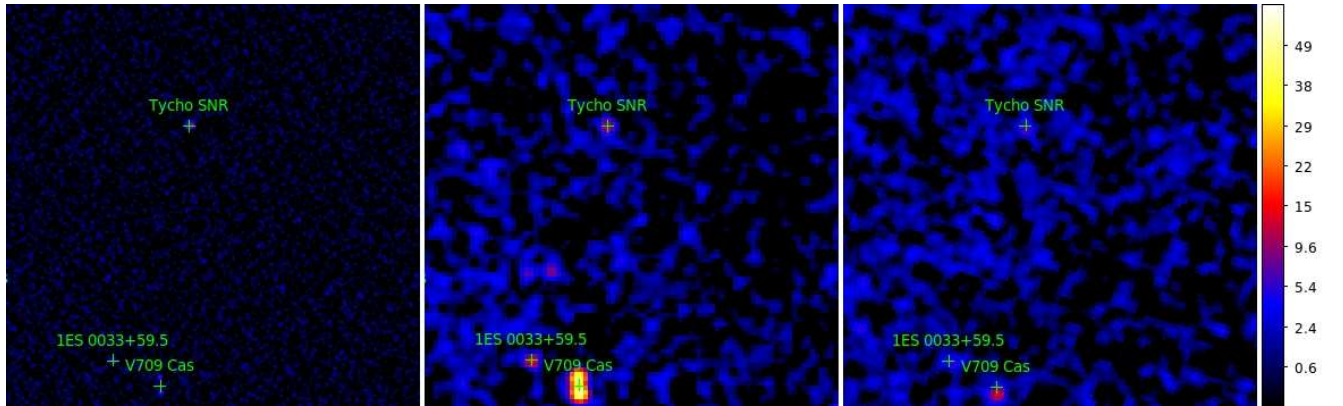


Fig. 1.— Significance mosaic maps ( $6^\circ \times 6^\circ$ ) around Tycho supernova remnant in Equatorial J2000 coordinates as seen with INTEGRAL/JEM-X (left) in the range of 3 – 10 keV and INTEGRAL/IBIS in the energy band of 20 – 60 keV (middle) and 60 – 90 keV (right). Tycho SNR was detected by JEM-X with a significance level of  $9.8\sigma$  and by IBIS with the significance levels of  $\sim 11.6\sigma$  and  $5\sigma$  in two energy bands, respectively.

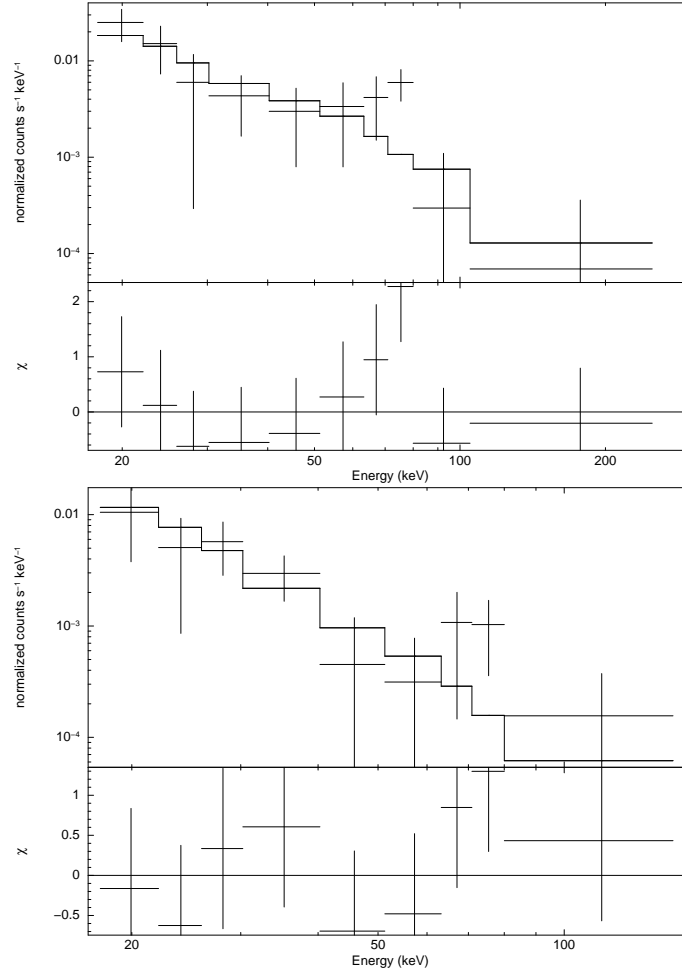


Fig. 2.— IBIS/ISGRI hard X-ray spectra of Tycho SNR for two different datasets and the associated best-fit power-law models. **Top:** data from Rev. 331 to 396 with  $\Gamma = 2.5 \pm 0.4$  (reduced  $\chi^2 \sim 1.23$ , 8 d.o.f). **Bottom:** data from Rev. 883 to 1066 with  $\Gamma = 2.9 \pm 0.5$  (reduced  $\chi^2 \sim 1.13$ , 7 d.o.f).

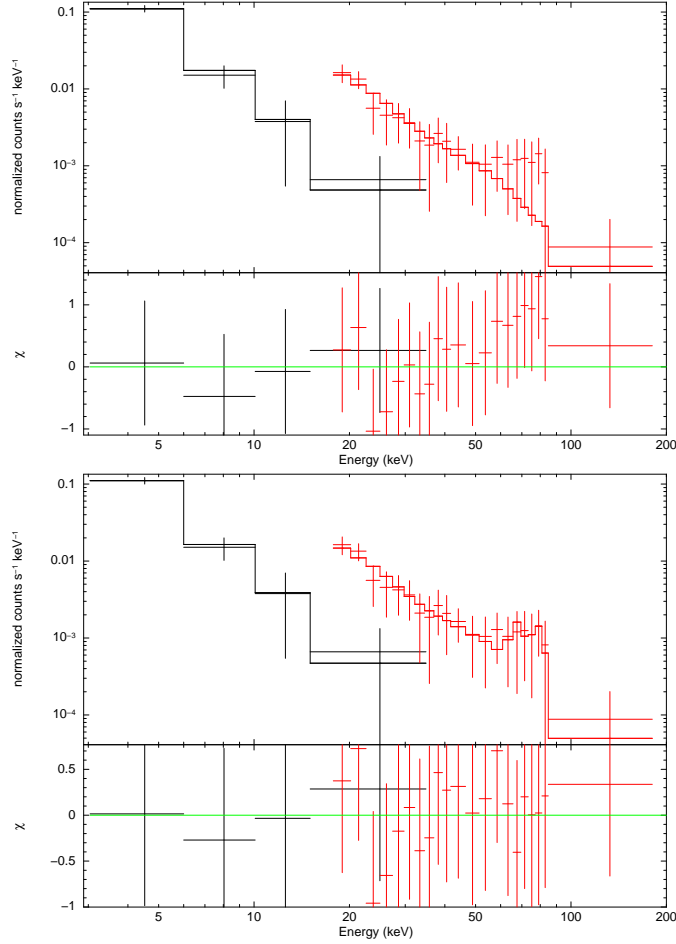


Fig. 3.— **Top:** The spectrum of the Tycho SNR in hard X-ray band of 3 – 200 keV. The spectrum is fitted with a thermal bremsstrahlung of  $kT \sim 0.92 \pm 0.48$  keV plus a power-law model of  $\Gamma \sim 3.02 \pm 0.14$ , reduced  $\chi^2 = 1.251$  (22 *d.o.f.*). The continuum flux of 3 – 100 keV is  $\sim (8.5 \pm 0.5) \times 10^{-11}$  erg cm<sup>-2</sup> s<sup>-1</sup>. **Bottom:** The spectrum of the Tycho SNR with two <sup>44</sup>Ti emission lines at  $\sim 68$  and 78 keV fitted. See the text for details.

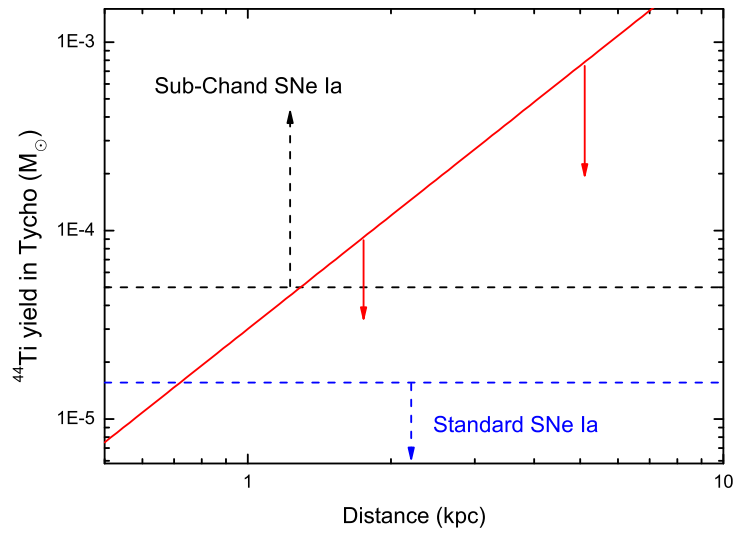


Fig. 4.— The derived  $^{44}\text{Ti}$  yield upper limit in Tycho as function of distance. The red solid line represents the upper limit function (a  $3\sigma$  upper limit of  $1.5 \times 10^{-5} \text{ ph cm}^{-2} \text{ s}^{-1}$ ) of the  $^{44}\text{Ti}$  yield. The figure also displays the calculated  $^{44}\text{Ti}$  yield ranges from the 2D and 3D simulation results of standard Chandrasekhar mass (about  $1.4M_{\odot}$ , Maeda et al. 2010; Seitenzahl et al. 2013) and sub-Chandrasekhar mass models (Woosley & Kasen 2011) of Type Ia supernovae.